Exceptional Response to Temsirolimus in a Metastatic Clear Cell Renal Cell Carcinoma With an Early Novel *MTOR*-Activating Mutation

Juan Francisco Rodríguez-Moreno, MD[a,b,*]; María Apellaniz-Ruiz, PhD[c,*]; Juan María Roldan-Romero, MS[c]; Ignacio Durán, MD[d]; Luis Beltrán, MD[e]; Cristina Montero-Conde, PhD[c]; Alberto Cascón, PhD[c,f]; Mercedes Robledo, PhD[c,f]; Jesus García-Donas, MD, PhD[a,b,†]; and Cristina Rodríguez-Antona, PhD[c,f,†]

Abstract

mTOR pathway inhibitors are important drugs for the treatment of advanced renal cell carcinoma (RCC). However, no valid predictive markers have been identified to guide treatment selection and identify patients who are sensitive to these drugs. Mutations activating the mTOR pathway have been suggested to predict response; however, their predictive value is still unclear. Here, we present the genomic and functional characterization of a patient with metastatic clear cell RCC (ccRCC) who experienced a partial response to temsirolimus after a poor response to 2 previous lines of treatment. At the time of publication, the patient was disease-free 8 years after temsirolimus treatment. Multiregion whole-exome sequencing (WES) on 3 regions of the primary tumor, 1 metastasis, and blood revealed tumor mutations in driver genes in ccRCC: a missense mutation in *VHL* (p.W88L), a loss-of-function mutation in *BAP1* (p.E454Rfs*15), and a novel missense mutation in *MTOR* (p.Y1974H). The *MTOR* mutation was present in all tumor regions, with similar allele frequency as the *VHL* mutation, and in vitro functional assessment of the *MTOR* variant demonstrated that it increased mTORC1 activity. Consistently, immunohistochemistry in the tumor samples demonstrated increased levels of phospho-S6. In conclusion, multiregion WES identified a novel *MTOR* mutation acquired early during tumor development as the event leading to a high sensitivity to temsirolimus treatment. This study supports tumor multiregion sequencing to detect truncal mutations in the mTOR pathway to identify patients sensitive to mTOR inhibitors.

J Natl Compr Canc Netw 2017;15(11):1310–1315
doi: 10.6004/jnccn.2017.7018

Treatment of advanced renal cell carcinoma (RCC) has changed drastically in the past decade. The mTORC1 inhibitors, everolimus and temsirolimus (also known as *rapalogs*), have been shown to be key drugs for use in first-line treatment[1] and pretreated patients.[2] Although recent evidence showed they had inferior global efficacy compared with modern immunotherapy[3] or new targeted agents,[4] approximately 20% of all patients with RCC respond to rapalogs. Furthermore, mTOR inhibitors combined with novel antiangiogenic agents have become a standard of care in pretreated patients,[5,6] and ongoing trials are exploring the value of these combinations in first-line treatment (ClinicalTrials.gov identifier: NCT02811861).

From [a]Oncology Unit, Clara Campal Comprehensive Cancer Center, Madrid, Spain; [b]Spanish Oncology GenitoUrinary Group (SOGUG), Madrid, Spain; [c]Hereditary Endocrine Cancer Group, Human Cancer Genetics Programme, Spanish National Cancer Research Centre (CNIO), Madrid, Spain; [d]Instituto de Biomedicina de Sevilla, IBiS/Hospital Universitario Virgen del Rocío/CSIC/Universidad de Sevilla, Sevilla, Spain; [e]Department of Surgery, Whipps Cross Hospital, London, United Kingdom; and [f]Centro de Investigación Biomédica en Red de Enfermedades Raras (CIBERER), Madrid, Spain.

*These authors contributed equally.

†These authors acted as senior authors.

Submitted March 15, 2017; accepted for publication August 2, 2017.

The authors have disclosed that they have no financial interests, arrangements, affiliations, or commercial interests with the manufacturers of any products discussed in this article or their competitors.

This study was supported by Projects SAF2015-70820-ERC and SAF2015-64850-R (Spanish Ministry of Economy, Industry and Competitiveness MEIC, co-funded by the European Regional Development Fund ERDF) and by the Instituto de Salud Carlos III (Acción Estratégica en Salud grant number PI13/00622).

Correspondence: Cristina Rodríguez-Antona, PhD, Spanish National Cancer Research Centre (CNIO), Hereditary Endocrine Cancer Group, Melchor Fernández Almagro 3, 28029 Madrid, Spain.
E-mail: crodriguez@cnio.es;

Jesus García-Donas, MD, Clara Campal Comprehensive Cancer Center, Oncology Unit, Oña Street 10, 28050 Madrid, Spain.
E-mail: jgarciadonas@gmail.com

Extraordinary responses to mTOR inhibitors have been described in few patients with mutations in *TSC1*, *TSC2*, or *MTOR*.[7–9] However, a recent study in RCC showed that not all patients with mTOR-activating mutations responded to hh inhibitors, whereas some without mutations did.[10] Additionally, Lim et al[11] explored *MTOR*, *TSC1*, *TSC2*, *NF1*, and *PIK3CA* mutations in a cohort of 22 patients with different tumors with significant response to everolimus, identifying candidate mutations in only 50%. These studies suggest that additional mechanisms, such as clonal heterogeneity,[12,13] modulate response. Thus, understanding of the underlying mechanisms leading to mTOR inhibitor tumor sensitivity is currently incomplete, and additional investigations and cases demonstrating exquisite responses are needed.

This study describes a patient with metastatic clear cell RCC (ccRCC) refractory to multiple lines of anti–vascular endothelial growth factor (VEGF) therapy that, on temsirolimus treatment, exhibited an exceptional clinical response. Multiregional whole-exome sequencing (WES), in vitro functional assessment, and immunohistochemistry (IHC) of the tumor samples identified a novel *MTOR* mutation acquired early during tumor development as being responsible for the drug sensitivity. The molecular characterization of patients experiencing long responses to rapalogs could help define a subset who would benefit from these drugs.

Case Report

A 57-year-old Caucasian woman with an unremarkable past medical history presented with lumbar pain. Physical examination revealed a mass on the right flank. An FDG-PET scan revealed a renal mass highly suggestive of malignancy, signs of liver spread, and pelvic and lumbar spinal cord bone metastases (Figure 1A). Tumor staging at initial diagnosis was pT1bN0M1 (stage IV). In April 2007, an open right radical nephrectomy was performed. The histopathologic report revealed Fuhrman grade 4 advanced ccRCC. According to the Memorial Sloan Kettering Cancer Center (MSKCC) prognostic model,[14] the patient was classified as being in the intermediate-risk group based on 2 risk factors for the prognostic score: Karnofsky performance status of 70% and a serum lactic dehydrogenase level >1.5 times the upper limit of normal. She received palliative radiotherapy for a painful right iliac metastasis and started sunitinib treatment at 50 mg/d on a 4 weeks on, 2 weeks off schedule (4/2). After 2 cycles, all tumoral lesions had progressed and treatment was switched to sorafenib, 400 mg twice daily. New response assessment after 2 cycles revealed disease progression with new liver and bone lesions and clinical deterio-

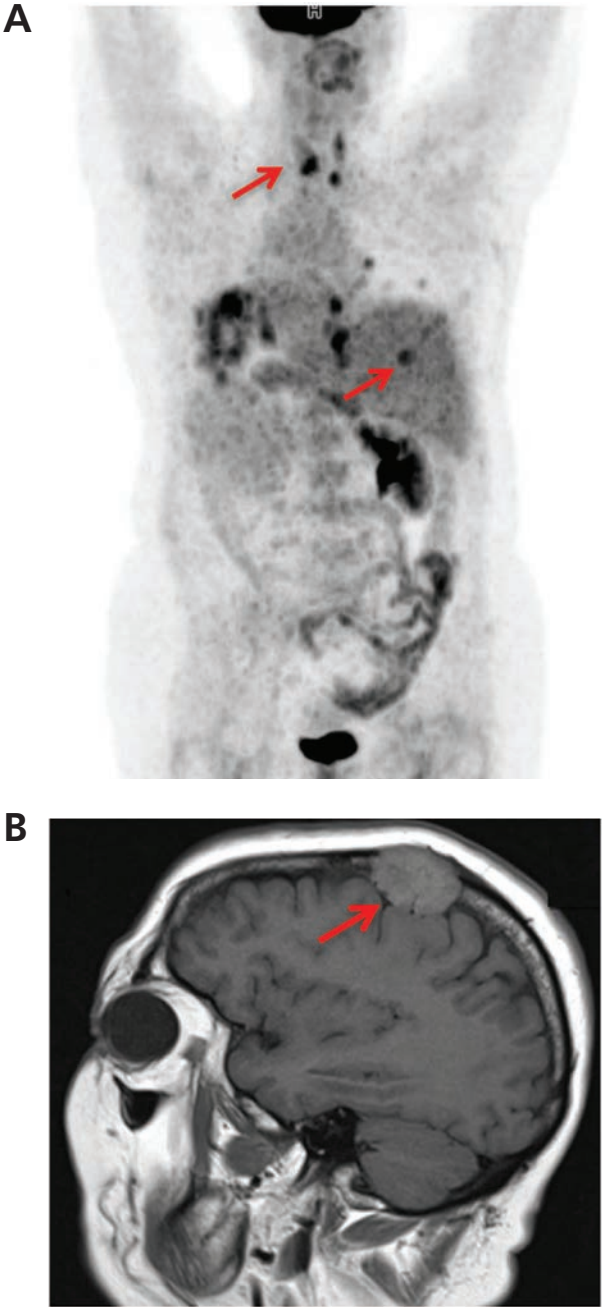

Figure 1. (A) Initial tumor dissemination detected by PET/CT (arrows). (B) MRI showing skull metastasis (arrow), which was surgically removed in 2015.

ration. In March 2008, the patient started temsirolimus at 25 mg weekly and experienced a remarkable clinical benefit. She had a partial response according to RECIST criteria, with a time to best response after starting temsirolimus of 6 weeks (temsirolimus start: March 3, 2008; response at first reevaluation: April 16, 2008), and experienced overall good tolerance; she continued temsirolimus for >7 years. Main toxicity consisted of 3 different pneumonitis episodes (grade 1–3) that required dose interruptions or reductions. In August 2015, a new solitary bone metastasis arose in the skull, whereas others remained with no change (Figure 1B). A complete resection of the lesion was performed followed by local radiotherapy. At 21 months after the metastasectomy, the patient continues on treatment with biweekly temsirolimus in combination with denosumab, with no tumor progression.

We performed WES in 3 different regions of the primary tumor obtained before treatment, in the skull metastasis resected 7 years after temsirolimus treatment initiation, and in the germline DNA obtained from the patient's blood. The mean depth of coverage was >80x for the 3 regions of the primary tumors, 136x for the metastasis, and 94x for the blood (see supplemental eAppendix 1 for details regarding methodology, available online with this article at JNCCN.org). The number of tumor mutations (single nucleotide variants and indels) leading to nonsynonymous coding or loss-of-function (LOF) variants in the primary tumor was 160. Tumor mutations refer to those detected in the tumor but absent in the blood. In total, 116, 76, and 65 mutations were detected in each of the 3 tumor regions and from these, 41 were shared (Figure 2; supplemental eTable 1). Among the shared tumor mutations, 39 were missense variants and 2 were LOF variants caused by frameshifts. The variants affecting genes frequently mutated in ccRCC were detected in all tumor samples analyzed: *VHL* (c.263G>T; p.W88L), *BAP1* (c.1359dup; p.E454Rfs*15), and *MTOR* (c.5920T>C; p.Y1974H), and were validated by Sanger sequencing. In ccRCC the primary driver event is *VHL* inactivation, and thus *VHL* mutations are early alterations present in all tumor cells.[15] The *MTOR* mutation frequencies detected in the different tumor samples sequenced were similar to those found for *VHL*, indicating that the *MTOR* mutation was also a truncal event in this patient (average ratio

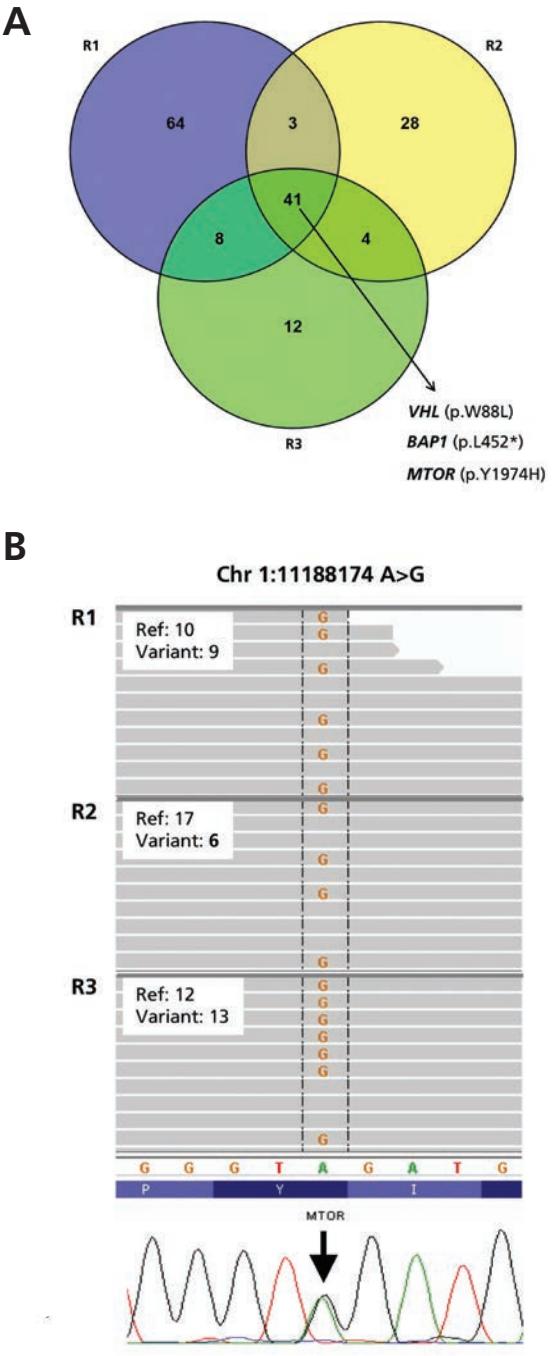

Figure 2. Mutations revealed by whole-exome sequencing (WES). (A) Venn diagram indicating the number of tumor (absent in blood) loss-of-function and nonsynonymous coding variants identified through WES in 3 regions (R1–R3) of the primary tumor. Shared variants affecting relevant clear cell renal cell carcinoma genes are indicated below the arrow. (B) Representative genome images from the Integrative Genomics Viewer (Broad Institute), along with the number of reads for the reference (ref) and variant allele of the *MTOR* Y1974H mutation, and Sanger sequencing chromatogram.

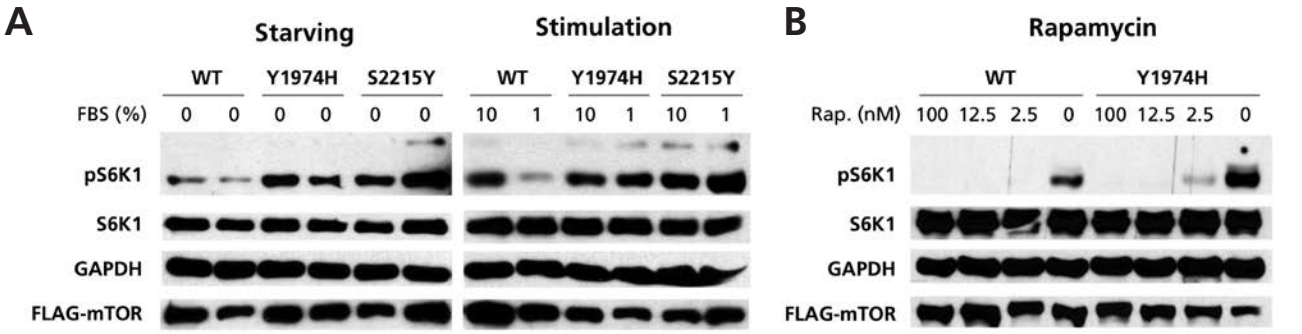

Figure 3. Functional assessment of *MTOR* p.Y1974H variant. Constructs expressing wild-type (WT) mTOR, mTOR Y1974H, and mTOR S2215Y (a positive control for mTOR activation) were transfected in HEK293 cells and the effect of phosphorylation of the downstream target S6K1 (pS6K1) was tested with Western blot. (A) Western blot analysis 24 hours after transfection cells were serum-starved for 24 hours (Starving) and then stimulated with 1% or 10% fetal bovine serum for 2 hours (Stimulation). In the Starving assay, lanes 1–2, 3–4, and 5–6 are duplicates from different experiments. (B) Cells transfected with *mTOR* constructs were treated with 2.5, 12.5, and 100 nM of rapamycin (rap) for 6 hours.
Abbreviation: GAPDH, glyceraldehyde 3-phosphate dehydrogenase.

of 1.1; supplemental eTable 1). For *BAP1* mutation, the average ratio was 0.66. Other genes implicated in cancer with mutations included *BCL11B*, *CIC*, *EML4*, *KMT2C*, *NOTCH1*, and *RANBP2* (see supplemental eTable 1).

To assess the effect of the *MTOR* novel variant p.Y1974H, HEK293 cells were transfected with constructs expressing the wild-type mTOR protein or the Y1974H variant protein. The mTOR-activating mutation S2215Y was used as control for the experiments. The Thr389 phospho-S6K1 (pS6K1) levels, which represent TORC1 activity, were augmented for the Y1974H variant compared with mTOR wild-type, and similar to those obtained for S2215Y (Figure 3A), indicating that mTOR Y1974H activates mTORC1. In addition, we observed that mTOR Y1974H was sensitive to rapamycin (Figure 3B). mTOR Y1974H also led to an increased number of cells in S phase with a concomitant decrease in G0/G1, and an alteration in forward scatter (data related to an alteration in cell size) compared with mTOR wild-type and similar to mTOR S2215Y (supplemental eFigure 1).[16] Immunohistologic analysis of the tumor samples revealed activation of the mTOR pathway through a positive immunostaining of phospho-S6, a downstream target of mTOR (Figure 4A–C), with the metastasis staining being more intense than that in the primary tumor. The staining of p-ERK (Figure4 D–F) was weak in the primary tumor, whereas the metastasis exhibited a nuclear and cytoplasmatic intense and extensive staining.

WES of the metastasis that arose 7 years after starting temsirolimus treatment revealed 80 tumor nonsynonymous coding or LOF variants (71 missense, 2 in-frame deletions, and 7 LOF) present in the tumor and absent in the blood. Of these, 51 were shared with the primary tumor and 29 were exclusively present in the metastasis (supplemental eTable 1). Among the genes exclusively mutated in the metastasis, only 3 (*CRTC3*, *KAT6B*, *PBRM1*) were in the Cancer Gene Census (CGC) but none were directly related to the *MTOR* pathway, and the variants have not been previously described in tumors, according to the COSMIC database.

The full region of the *MTOR* FKBP-rapamycin binding domain (FRB), including intronic regions, was sequenced by Sanger. However, no metastasis-specific variants were detected.

Discussion

Rapalogs are drugs approved for metastatic ccRCC in first-line treatment[1] and pretreated patients.[2] Although recent studies have shown less efficacy of rapalogs compared with nivolumab[3] and cabozantinib,[4] combination of everolimus and lenvatinib has become a second-line standard,[5,6] and ongoing trials are assessing combinations in first-line treatment. Interestingly, monotherapy with mTOR inhibitors is very useful in a considerable subgroup of patients, with long-term responses, regardless of the line of treatment.[10,12] Mutations affecting mTOR pathway genes have been explored as possible biomarkers of activity for these drugs, and despite initial descriptions of highly sensitive patients with mutations in *MTOR*, *TSC1*, and *TSC2*,[7–9] more recent studies show only

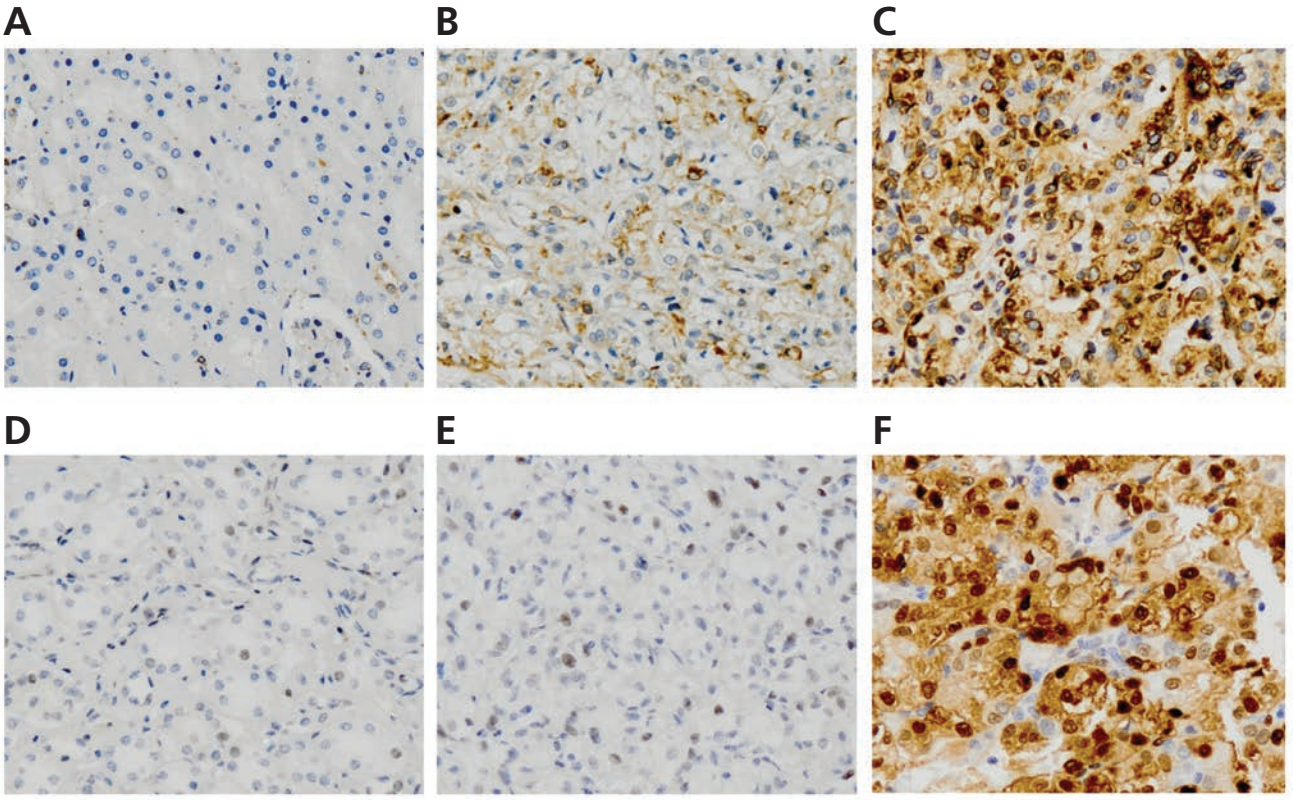

Figure 4. Immunohistochemical (IHC) study of *TSC2* and phospho-S6. Representative pictures of phospho-S6 IHC staining (original magnification x20) in (A) nontumoral kidney, (B) primary tumor, and (C) bone metastasis from the patient. Phospho-ERK staining (original magnification x20) in (D) nontumoral kidney, (E) primary tumor, and (F) bone metastasis.

partial correspondence between mTOR pathway mutations and response to mTOR inhibitors.[10] Thus, understanding of the molecular mechanisms conferring sensitivity to mTOR drugs is incomplete, and it is crucial to identify biomarkers that would allow tailored treatment of advanced RCC.

This report presents a patient with metastatic ccRCC who experienced an unusual prolonged response to temsirolimus. Multiregion sequencing of the tumor, functional studies on a candidate variant, and immunohistologic characterization of the tumors allowed the identification of an *MTOR* mutation (p.Y1974H) as causative for the response. This mutation is located in the FAT (FRAP-ATM-TTRAP) domain of mTOR, a region that has a prominent cluster of hyperactivating mutations in RCC that lead to an increase in mTORC1 and mTORC2 activities.[17,18] These mutations may destabilize the structure of the FAT domain, directly deregulating mTOR kinase activity and affecting the binding of mTOR complex proteins.[18] As expected for ccRCC, a *VHL* mutation (p.W88L) was found in all regions of the primary tumor and in the metastasis, in agreement with an early event.[15,19] Additional alterations in genes frequently mutated in clear cell histology were present in *BAP1* and *MTOR*.[20] The *MTOR* mutation (p.Y1974H) was detected in the 3 regions of the primary tumor and in the metastasis with similar frequency to *VHL* mutation, the major ccRCC driver event (supplemental eTable 1), and functional in vitro assays confirmed it was an activating mutation. ccRCC intratumor heterogeneity has been shown to affect the mTOR pathway,[15] and the moment during clonal evolution in which the mutations occur has been suggested to impact drug response.[12,13] Our results are consistent with a truncal *MTOR* mutation, which would render the tumor ubiquitously addicted to mTORC1 hyperactivity. In addition, the *BAP1* mutation found in the patient suggested a poor outcome, because these mutations are associated with poor RCC prognosis.[21,22] The remarkable response obtained with third-line temsirolimus highlights the high sensitivity to this drug.

Interestingly, the patient developed a bone metastasis while receiving temsirolimus. To date, there is one report identifying a mechanism for acquired mTOR inhibitor resistance, which consisted of a secondary mutation (p.F2108L) in mTOR FRB domain.[9] In the present patient, the only *MTOR* mutation found in the metastasis was p.Y1974H. Sequencing of the intronic region of *MTOR* FRB domain ruled out mutations that may lead to alternative splicing events altering this region. Regarding other genes, WES revealed mutations exclusive of the metastasis; however, none of the mutated genes was directly related to the mTOR pathway. IHC of the tumors revealed more intense staining for phospho-S6 in the metastasis than in the primary tumor, suggesting that the metastasis had acquired an additional alternative mechanism hyperactivating mTORC1. Phospho-ERK–strong IHC staining in the metastasis (Figure 4F) suggested the mechanism could be connected with the Ras-ERK pathway; however, none of the metastasis mutations were directly linked with this pathway. At any rate, the resistance mechanism may involve alterations not detectable by DNA sequencing (eg, epigenetic changes).

Conclusions

Although patients with extraordinary responses to mTOR inhibitors have been reported, the mechanisms underlying these responses are still not well understood. In this study, multiregional WES directly linked a truncal novel activating *MTOR* mutation with the exceptional response to temsirolimus in a patient with ccRCC. Our results support the sequencing of multiple tumor areas to identify early mutations affecting the mTOR pathway, to ultimately reveal predictive markers able to personalize RCC treatments.

Acknowledgments

The authors would like to thank the National Centre for Genomic Analysis personnel, and especially Sergi Beltran and Sophia Derdak, for their excellent support in whole-exome sequencing. They also want to thank the CNIO Flow Cytometry Core Unit and Dolores Martinez for their excellent support and assistance.

References

1. Hudes G, Carducci M, Tomczak P, et al. Temsirolimus, interferon alfa, or both for advanced renal-cell carcinoma. N Engl J Med 2007;356:2271–2281.
2. Motzer RJ, Escudier B, Oudard S, et al. Phase 3 trial of everolimus for metastatic renal cell carcinoma: final results and analysis of prognostic factors. Cancer 2010;116:4256–4265.
3. Motzer RJ, Escudier B, McDermott DF, et al. Nivolumab versus everolimus in advanced renal-cell carcinoma. N Engl J Med 2015;373:1803–1813.
4. Choueiri TK, Escudier B, Powles T, et al. Cabozantinib versus everolimus in advanced renal-cell carcinoma. N Engl J Med 2015;373:1814–1823.
5. Motzer RJ, Hutson TE, Glen H, et al. Lenvatinib, everolimus, and the combination in patients with metastatic renal cell carcinoma: a randomised, phase 2, open-label, multicentre trial. Lancet Oncol 2015;16:1473–1482.
6. Motzer RJ, Hutson TE, Ren M, et al. Independent assessment of lenvatinib plus everolimus in patients with metastatic renal cell carcinoma. Lancet Oncol 2016;17:e4–5.
7. Iyer G, Hanrahan AJ, Milowsky MI, et al. Genome sequencing identifies a basis for everolimus sensitivity. Science 2012;338:221.
8. Wagle N, Grabiner BC, Van Allen EM, et al. Activating *MTOR* mutations in a patient with an extraordinary response on a phase I trial of everolimus and pazopanib. Cancer Discov 2014;4:546–553.
9. Wagle N, Grabiner BC, Van Allen EM, et al. Response and acquired resistance to everolimus in anaplastic thyroid cancer. N Engl J Med 2014;371:1426–1433.
10. Kwiatkowski DJ, Choueiri TK, Fay AP, et al. Mutations in TSC1, TSC2, and *MTOR* are associated with response to rapalogs in patients with metastatic renal cell carcinoma. Clin Cancer Res 2016;22:2445–2452.
11. Lim SM, Park HS, Kim S, et al. Next-generation sequencing reveals somatic mutations that confer exceptional response to everolimus. Oncotarget 2016;7:10547–10556.
12. Voss MH, Hakimi AA, Pham CG, et al. Tumor genetic analyses of patients with metastatic renal cell carcinoma and extended benefit from *MTOR* inhibitor therapy. Clin Cancer Res 2014;20:1955–1964.
13. Voss MH, Hsieh JJ. Therapeutic guide for mTOuRing through the braided kidney cancer genomic river. Clin Cancer Res 2016;22:2320–2322.
14. Motzer RJ, Bacik J, Mazumdar M. Prognostic factors for survival of patients with stage IV renal cell carcinoma: Memorial Sloan-Kettering Cancer Center experience. Clin Cancer Res 2004;10:6302S–6303S.
15. Gerlinger M, Horswell S, Larkin J, et al. Genomic architecture and evolution of clear cell renal cell carcinomas defined by multiregion sequencing. Nat Genet 2014;46:225–233.
16. Sato T, Nakashima A, Guo L, et al. Single amino-acid changes that confer constitutive activation of *MTOR* are discovered in human cancer. Oncogene 2010;29:2746–2752.
17. Grabiner BC, Nardi V, Birsoy K, et al. A diverse array of cancer-associated *MTOR* mutations are hyperactivating and can predict rapamycin sensitivity. Cancer Discov 2014;4:554–563.
18. Ghosh AP, Marshall CB, Coric T, et al. Point mutations of the *MTOR*-RHEB pathway in renal cell carcinoma. Oncotarget 2015;6:17895–17910.
19. Gerlinger M, Rowan AJ, Horswell S, et al. Intratumor heterogeneity and branched evolution revealed by multiregion sequencing. N Engl J Med 2012;366:883–892.
20. TCGA. Comprehensive molecular characterization of clear cell renal cell carcinoma. Nature 2013;499:43–49.
21. Pena-Llopis S, Vega-Rubin-de-Celis S, Liao A, et al. BAP1 loss defines a new class of renal cell carcinoma. Nat Genet 2012;44:751–759.
22. Kapur P, Pena-Llopis S, Christie A, et al. Effects on survival of BAP1 and PBRM1 mutations in sporadic clear-cell renal-cell carcinoma: a retrospective analysis with independent validation. Lancet Oncol 2013;14:159–167.

See JNCCN.org for supplemental online content.

Gene	Variant	Ref. allele	Alt. Allele	Primary T1_AF	Primary T2_AF	Primary T3_AF	Metastasis_AF	Effect	Amino_Acid_Change	Transcript_ID
ACACB	12:109670522	C	A	0.31	0.20	0.22	0.33	MISSENSE	S1280R;S1350R;S1350R	ENST00000377854;ENST00000338432;ENST00000377848
ADAL	15:43643188	C	A	0.36	0.18	0.32	0.31	MISSENSE	D274E;D274E	ENST00000422466;ENST00000562188
ADAM28	8:24181384	G	A	0.17				MISSENSE	G253D	ENST00000265769
ADAMTSL4	1:150526429	G	A	0.20				MISSENSE	G321E;G321E;G321E	ENST00000271643;ENST00000369038;ENST00000369039
AJAP1	1:4772367	C	T		0.17			MISSENSE	P146L;P146L	ENST00000378190;ENST00000378191
AK2	1:33487194	C	T	0.17				MISSENSE	M110I;M110I;M110I	ENST00000373449;ENST00000467905;ENST00000354858
ALS2CR11	2:202358161	C	T	0.20				MISSENSE	G968E	ENST00000439140
ANKRD18B	9:33541216	G	C	0.33	0.23	0.24		MISSENSE	G294R	ENST00000290943
AP001468.1	21:47613570	T	C	0.45	0.31			MISSENSE	H35R	ENST00000594486
APOBEC3C	22:39411749	G	A		0.22			MISSENSE	R56Q	ENST00000361441
ARHGAP22	10:49658586	C	A		0.27			MISSENSE	C529F;C535F;C545F	ENST00000249601;ENST00000435790;ENST00000417912
ARID2	12:46245092	G	T	0.36	0.28	0.41	0.28	MISSENSE	Q1062H	ENST00000334344
ARL14EP	11:30352649	G	A	0.23				MISSENSE	G52R	ENST00000282032
ARMC4	10:28250610	C	A		0.29	0.24	0.14	MISSENSE	D425Y	ENST00000305242
ARX	X:25025243	C	G	0.64	0.48	0.42	0.57	MISSENSE	S478T	ENST00000379044
ATHL1	11:289880	C	G	0.44	0.33	0.51	0.38	MISSENSE	L22V;L22V	ENST00000409548;ENST00000409479
ATP9B	18:76886357	AG	A	0.26		0.21	0.21	FRAME_SHIFT		ENST00000307671
BAP1	3:52437801	CTTT	CTTTT	0.34	0.16	0.28	0.26	FRAME_SHIFT		ENST00000460680
BCL11B	14:99641956	G	A	0.27				MISSENSE	T212M;T335M;T406M	ENST00000443726;ENST00000345514;ENST00000357195
BSCL2	11:62472862	C	A	0.39	0.18	0.19	0.40	MISSENSE	L105F;L105F;L105F;L41F;L41F;L41F;L41F;L41F	ENST00000360796;ENST00000433053;ENST00000405837;ENST00000278893;ENST00000403550;ENST00000407022;ENST00000421906
C4orf21	4:113539720	G	A	0.18				MISSENSE	S493F	ENST00000505019
C7orf55-LUC7L	7:139092020	G	T	0.26	0.16	0.25	0.30	MISSENSE	R204I;R270I	ENST00000354926;ENST00000541515
CARD16	11:104915222	C	A		0.18			MISSENSE	L57F;L57F;L57F	ENST00000375706;ENST00000375704;ENST00000525374
CCNG1	5:162868187	G	A	0.13				MISSENSE	R123Q;R123Q	ENST00000340828;ENST00000393929
CDC14B	9:99296337	A	T	0.38	0.22	0.24	0.51	MISSENSE	F273Y;F273Y;F273Y	ENST00000375236;ENST00000463569;ENST00000375241
CELF2	10:11259399	G	A			0.22		MISSENSE	V64I;V64I;V64I;V64I;V64I;V64I	ENST00000417956;ENST00000608830;ENST00000315874;ENST00000354440;ENST00000399850;ENST00000427450
CFH	1:196715027	G	A	0.20				MISSENSE	A1131T	ENST00000367429
CHUK	10:101950628	T	A	0.42	0.29	0.34	0.34	MISSENSE	M736L	ENST00000370397
CIC	19:42795216	G	T	0.15				MISSENSE	G1675C;G766C;G766C	ENST00000572681;ENST00000160740;ENST00000575354
CILP2	19:19656719	C	T			0.16		MISSENSE	P1122L;P1128L	ENST00000291495;ENST00000586018
CKAP5	11:46786695	C	A	0.20				NONSENSE	E1175*	ENST00000529230
CLSPN	1:36219445	T	G	0.39	0.24	0.30	0.20	MISSENSE	K558Q;K558Q;K558Q	ENST00000520551;ENST00000251195;ENST00000318121
CNKSR1	1:26511636	G	A		0.15			MISSENSE	V423M;V430M	ENST00000361530;ENST00000374253
CPNE2	16:57144689	C	T	0.57	0.32	0.29	0.19	MISSENSE	A12V;A12V;A12V	ENST00000290776;ENST00000535318;ENST00000565874
CTR9	11:10781764	A	G	0.37	0.20	0.18	0.24	MISSENSE	K213E	ENST00000361367
CTSH	15:79224788	T	G			0.14		MISSENSE	S140R	ENST00000220166
CXorf23	X:19971111	C	T	0.20				MISSENSE	E542K;E542K;E542K	ENST00000356980;ENST00000379687;ENST00000379682
CYP2A6	19:41355828	C	T	0.12				MISSENSE	V80M	ENST00000301141
DDX46	5:134131842	T	A	0.17				SPLICE_SITE_DONOR		ENST00000354283;ENST00000452510
DEF6	6:35286030	C	T		0.21			MISSENSE	R333W	ENST00000316637
DENND3	8:142185453	G	T	0.42	0.22	0.22	0.37	MISSENSE	K730N;K810N	ENST00000262585;ENST00000519811
DHRS4	14:24424266	C	T	0.25				MISSENSE	R51C	ENST00000313250
DHX30	3:47891435	T	A	0.46	0.33	0.42	0.56	MISSENSE	L1098Q;L1137Q	ENST00000446256;ENST00000445061
DHX40	17:57679913	G	T	0.18				MISSENSE	G613C	ENST00000251241
DIDO1	20:61512104	G	A	0.20				MISSENSE	P1735L;P1735L	ENST00000266070;ENST00000395343
DNAH6	2:85011924	A	T	0.43	0.24	0.34	0.32	MISSENSE	N3648I;N3648I	ENST00000237449;ENST00000389394
DOCK11	X:117676803	C	T	0.17				MISSENSE	S73F;S73F	ENST00000276202;ENST00000276204
EEA1	12:93226564	A	T	0.18				MISSENSE	N326K	ENST00000322349
EIF4G3	1:21268389	C	T	0.18				MISSENSE	E364K;E364K;E370K;E370K	ENST00000264211;ENST00000400422;ENST00000374937;ENST00000602326
EML4	2:42510010	C	T	0.19				MISSENSE	P222L;P280L;P291L	ENST00000402711;ENST00000318522;ENST00000401738
FCGBP	19:40424297	A	T	0.36	0.20	0.30	0.34	MISSENSE	F636I	ENST00000221347
FER1L6	8:124975587	T	C	0.29	0.25	0.34	0.23	MISSENSE	V49A;V49A	ENST00000399018;ENST00000522917
GAK	4:861013	G	A	0.20				MISSENSE	P868L	ENST00000314167
GLT6D1	9:138516493	G	A	0.23	0.24	0.32		MISSENSE	P94L	ENST00000371763
GOLPH3L	1:150620846	C	G	0.61	0.27	0.37	0.47	MISSENSE	S270T	ENST00000271732
HAS1	19:52216790	C	T	0.19				MISSENSE	A542T;A543T;A550T	ENST00000540069;ENST00000222115;ENST00000601714
HCAR3	12:123200354	G	A		0.69		0.38	MISSENSE	R311C	ENST00000528880
HLA-DOA	6:32975808	G	A	0.25	0.36	0.33	0.39	MISSENSE	R105C	ENST00000229829
HLA-DRB1	6:32549540	C	T	0.20	0.21	0.15		MISSENSE	S149N	ENST00000360004
HLA-DRB1	6:32549531	T	C			0.15		MISSENSE	Y152C	ENST00000360004
HLA-DRB1	6:32549525	C	G			0.15		MISSENSE	G154A	ENST00000360004
HNRNPLL	2:38812862	C	T	0.35		0.32	0.37	MISSENSE	G157E;G157E	ENST00000449105;ENST00000608859
HS6ST2	X:131842613	A	G			0.14		MISSENSE	M1T	ENST00000406696
HSD17B14	19:49316771	T	C	0.33	0.19	0.27	0.38	MISSENSE	E194G	ENST00000263278
IGHMBP2	11:68676003	G	T		0.15			MISSENSE	A151S	ENST00000255078
IGHV3-35	14:106845586	A	C	0.43	0.14			MISSENSE	L30V	ENST00000390617
IGHV3-35	14:106845579	T	C	0.30				MISSENSE	Q32R	ENST00000390617
INPP4B	4:143235912	G	A	0.19				NONSENSE	R126*;R126*;R126*;R126*	ENST00000262992;ENST00000308502;ENST00000508116;ENST00000513000
IRAK1	X:153284141	G	A	0.14				MISSENSE	S213L;S213L	ENST00000393687;ENST00000369980
KLHL20	1:173744950	C	T	0.21	0.21	0.14	0.27	MISSENSE	P536L	ENST00000209884
KLHL28	14:45414636	C	T	0.28	0.19	0.25	0.28	MISSENSE	A166T	ENST00000396128

KMT2C	7:151970856	T	A		0.44		0.24	MISSENSE	T316S;T316S	ENST00000262189;ENST00000355193
KRTAP10-2	21:45971109	G	A	0.19				MISSENSE	S78L	ENST00000391621
KRTAP4-11	17:39274087	G	C	0.50				MISSENSE	L161V	ENST00000391413
KRTAP4-6	17:39296361	A	G		0.21			MISSENSE	S127P	ENST00000345847
KRTAP4-8	17:39254013	G	C		0.17			MISSENSE	S108R	ENST00000333822
LACTB	15:63421702	C	T	0.18				MISSENSE	S324L	ENST00000261893
LILRA4	19:54848121	C	T	0.16	0.19			MISSENSE	V416M	ENST00000291759
LILRA4	19:54848157	A	G		0.15			MISSENSE	Y404H	ENST00000291759
LRCH2	X:114468558	C	T	0.20				MISSENSE	C16Y;C16Y	ENST00000538422;ENST00000317135
LYPLA2	1:24121214	C	T	0.46				MISSENSE	P230S	ENST00000374514
MBLAC1	7:99725466	G	T		0.20			MISSENSE	G150C	ENST00000398075
MINK1	17:4784282	C	T		0.17			MISSENSE	R43W;R43W;R43W	ENST00000347992;ENST00000453408;ENST00000355280
MLH3	14:75515080	C	A	0.17				MISSENSE	D427Y;D427Y;D427Y	ENST00000238662;ENST00000355774;ENST00000556740
MMP8	11:102584584	C	T	0.20				MISSENSE	D399N	ENST00000236826
MOBP	3:39544340	G	A	0.20				MISSENSE	G174E;G174E;G174E;G198E	ENST00000354668;ENST00000420739;ENST00000441980;ENST00000311042
MSL1	17:38285655	C	T		0.19			NONSENSE	Q121*	ENST00000579565
MTOR	1:11188174	A	G	0.47	0.26	0.52	0.48	MISSENSE	Y179H;Y1974H	ENST00000376838;ENST00000361445
MUC2	11:1093298	C	T			0.30		MISSENSE	T1706M	ENST00000441003
MYH8	17:10302118	T	A	0.20				MISSENSE	E1316D	ENST00000403437
NAT2	8:18258102	C	T	0.20				NONSENSE	R197*	ENST00000286479
NCAN	19:19337829	A	T			0.45	0.47	MISSENSE	Q536L	ENST00000252575
NEB	2:152364544	C	T		0.14			MISSENSE	R7809Q;R7809Q;R7809Q;R7809Q	ENST00000397345;ENST00000427231;ENST00000603639;ENST00000604864
NFE2	12:54686277	G	T	0.37	0.23	0.18	0.32	MISSENSE	Q335K;Q335K;Q335K;Q335K	ENST00000312156;ENST00000435572;ENST00000540264;ENST00000553070
NKTR	3:42678932	C	T	0.17				MISSENSE	P579L	ENST00000232978
NLGN4X	X:5811529	C	T		0.26			MISSENSE	V614I	ENST00000381093
NOTCH1	9:139396757	C	T	0.18				MISSENSE	R1784Q	ENST00000277541
OPN1SW	7:128413854	C	T	0.34	0.23	0.29	0.35	MISSENSE	C259Y	ENST00000249389
OR2T8	1:248084440	T	G	0.20				MISSENSE	S41A	ENST00000319968
OR8G5	11:124135536	G	A	0.17				MISSENSE	A272T	ENST00000524943
OSBP2	22:31301928	G	A	0.31	0.31	0.31	0.29	MISSENSE	R371Q;R460Q;R569Q;R654Q;R661Q;R778Q;R826Q;R827Q	ENST00000535268;ENST00000401475;ENST00000437268;ENST00000407373;ENST00000403222;ENST00000382310;ENST00000446658;ENST00000332585
PBRM1	3:52610615	G	T	0.18				NONSENSE	Y1179*;Y1211*;Y1211*;Y1211*;Y1226*	ENST00000356770;ENST00000337303;ENST00000409057;ENST00000296302;ENST00000409114
PCDH11X	X:91090772	G	A	0.21		0.21		MISSENSE	R90H;R90H;R90H;R90H;R90H;R90H;R90H;R90H;R90H;R90H	ENST00000361724;ENST00000395337;ENST00000504220;ENST00000298274;ENST00000373088;ENST00000361655;ENST00000373097;ENST00000406881;ENST00000373094
PCDHA12	5:140255334	G	A		0.17			MISSENSE	E93K	ENST00000398631
PCDHA13	5:140263541	C	T	0.45	0.31	0.31	0.22	MISSENSE	P563L	ENST00000289272
PCDHA8	5:140221195	G	C		0.27			MISSENSE	G97R;G97R	ENST00000378123;ENST00000531613
PCDHB15	5:140625864	C	T	0.39	0.24	0.21	0.22	MISSENSE	P240S	ENST00000231173
PCLO	7:82584389	T	A	0.17				MISSENSE	L1960F	ENST00000333891
PCNXL4	14:60591410	C	T	0.20				MISSENSE	H48Y;H607Y;H607Y;H841Y;H841Y	ENST00000535349;ENST00000406949;ENST00000317623;ENST00000404681;ENST00000406854
PITPNM1	11:67270189	T	C		0.18			MISSENSE	K27E;K27E;K27E	ENST00000436757;ENST00000356404;ENST00000534749
PLCG2	16:81990465	C	G	0.31	0.14	0.32	0.33	MISSENSE	Q1246E	ENST00000359376
PLEKHA5	12:19511369	C	A		0.24	0.54	0.40	MISSENSE	Q1008K;Q1008K;Q1013K;Q1116K;Q894K;Q950K	ENST00000355397;ENST00000538714;ENST00000317589;ENST00000429027;ENST00000359180;ENST00000299275
PNPLA7	9:140437947	G	A	0.16				MISSENSE	T123M;T148M	ENST00000277531;ENST00000406427
PODN	1:53535657	G	A	0.23				MISSENSE	E73K;E92K	ENST00000371500;ENST00000312553
PRSS3	9:33796673	G	A	0.15				MISSENSE	V25I	ENST00000379405
PSG1	19:43382305	C	T	0.18				MISSENSE	G64S;G64S;G64S;G64S	ENST00000595356;ENST00000436291;ENST00000244296;ENST00000312439
RAB11FIP5	2:73339583	A	G		0.17			MISSENSE	L108P	ENST00000258098
RAB24	5:176729430	A	C			0.37		MISSENSE	V134G;V134G	ENST00000303251;ENST00000393611
RANBP2	2:109399107	C	A	0.23		0.27	0.28	NONSENSE	S3053*	ENST00000283195
RASIP1	19:49242574	C	T		0.18			MISSENSE	A156T	ENST00000222145
RP11-166B2.1	16:12021361	G	A			0.20		MISSENSE	R355W	ENST00000399147
RP11-497E19.2	14:85995347	G	A	0.55		0.31	0.20	SPLICE_SITE_ACCEPTOR		ENST00000553678
RPH3AL	17:97000	G	A	0.42	0.38	0.37	0.43	MISSENSE	A172V	ENST00000331302
RPL32	3:12881657	C	T	0.36				MISSENSE	R27Q;R27Q;R27Q;R27Q	ENST00000396953;ENST00000396957;ENST00000429711;ENST00000435983
RXFP3	5:33936912	GAA	GA		0.16		0.23	FRAME_SHIFT		ENST00000330120
SAMD10	20:62607100	C	G		0.13			MISSENSE	Q177H	ENST00000369886
SEC22C	3:42602763	C	T	0.17				NONSENSE	W124*	ENST00000264454
SFMBT1	3:52966285	C	T	0.20				MISSENSE	G165R;G165R;G165R	ENST00000358080;ENST00000394750;ENST00000394752
SFTPB	2:85890886	A	G	0.30	0.20	0.33	0.34	MISSENSE	Y253H;Y253H;Y265H;Y265H	ENST00000342375;ENST00000519937;ENST00000393822;ENST00000409383
SNCAIP	5:121786359	G	A	0.18				MISSENSE	R606Q	ENST00000261368
SPAG5	17:26905093	C	T	0.18				MISSENSE	E1149K	ENST00000321765
SPATC1	8:145095304	C	T	0.30				MISSENSE	R236C;R236C	ENST00000447830;ENST00000377470
STAB1	3:52553984	C	T	0.25				NONSENSE	R1754*	ENST00000321725
STARD3	17:37817329	A	T	0.32		0.26		MISSENSE	K377I	ENST00000336308
STYXL1	7:75634688	ATTT	ATT	0.22	0.15	0.23	0.16	FRAME_SHIFT		ENST00000248600;ENST00000359697;ENST00000431581
SUPT20H	13:37622721	G	T		0.18			MISSENSE	L7I;L7I;L7I;L7I;L7I	ENST00000356185;ENST00000360252;ENST00000464744;ENST00000350612;ENST00000475892
SVIL	10:29756712	AAGGCATC	A	0.26		0.17	0.19	CODON_CHANGE_PLUS_CODON_DE	GFWDAL1548V;GFWDAL1974V;GFWDAL1974V;GFWDAL888	ENST00000375400;ENST00000355867;ENST00000375398;ENST00000535393
TAS2R10	12:10978260	G	T		0.14	0.18	0.34	MISSENSE	H203Q	ENST00000240619
TBX2	17:59477611	C	A	0.42	0.22	0.20	0.25	MISSENSE	P25H	ENST00000240328
TCIRG1	11:67812542	G	A		0.19			MISSENSE	V380M	ENST00000265686
TDRD1	10:115985973	A	C	0.37	0.22	0.29	0.26	MISSENSE	E1058A;E1058A;E1058A	ENST00000369280;ENST00000369282;ENST00000251864
TEKT3	17:15207296	C	T		0.13			MISSENSE	R477H;R477H	ENST00000338696;ENST00000395930
TLR1	4:38800221	G	C	0.20				MISSENSE	H78D;H78D	ENST00000308979;ENST00000502213

TMEM168	7:112407695	G	C	0.18	0.13	0.29	0.30	MISSENSE	P551A;P551A	ENST00000312814;ENST00000454074
TNFRSF11B	8:119936660	C	G	0.20				MISSENSE	E387Q	ENST00000297350
TPTE2	13:20000614	T	A	0.25				MISSENSE	Y338F;Y338F;Y372F;Y372F;Y409F;Y409F;Y449F;Y449F	ENST00000400103;ENST00000457266;ENST00000255310;ENST00000390680;ENST00000382975;ENST00000382978;ENST00000382977;ENST00000400230
TPTE2	13:20000621	T	C	0.17				MISSENSE	N336D;N336D;N370D;N370D;N407D;N407D;N447D;N447D	ENST00000400103;ENST00000457266;ENST00000255310;ENST00000390680;ENST00000382975;ENST00000382978;ENST00000382977;ENST00000400230
TRIM37	17:57139927	C	T	0.27				SPLICE_SITE_DONOR		ENST00000262294;ENST00000393066
TRIM56	7:100732488	G	A		0.20			MISSENSE	R632Q	ENST00000306085
TRMT6	20:5925530	T	C	0.40		0.40	0.40	MISSENSE	N96S	ENST00000203001
USP9X	X:41043260	C	T	0.17				MISSENSE	T1053M;T1053M	ENST00000378308;ENST00000324545
VHL	3:10183794	G	T	0.61	0.21	0.40	0.41	MISSENSE	W88L	ENST00000256474
WDR72	15:53907926	C	T	0.17				MISSENSE	G823D;G826D;G826D	ENST00000557913;ENST00000360509;ENST00000396328
WNK3	X:54359601	G	C	0.15				MISSENSE	T169R;T169R;T169R	ENST00000375169;ENST00000354646;ENST00000375159
XKR9	8:71593334	G	T			0.22		MISSENSE	G14V;G14V	ENST00000408926;ENST00000520030
ZDHHC11	5:837553	C	G		0.16	0.29		MISSENSE	R276P;R276P	ENST00000283441;ENST00000424784
ZNF208	19:22154249	A	G	0.24				MISSENSE	L1196P	ENST00000397126
ZNF429	19:21720618	G	C	0.15				MISSENSE	S588T	ENST00000358491
ZNF596	8:195911	G	A			0.25		MISSENSE	R285Q;R355Q;R355Q	ENST00000320552;ENST00000308811;ENST00000398612
ZNF85	19:21131682	T	C	0.41	0.18	0.21	0.44	MISSENSE	M121T;M88T	ENST00000328178;ENST00000345030
ACAP3	1:1231187	G	A				0.27	MISSENSE	P545L	ENST00000354700
CLEC18B	16:74447514	T	C				0.13	MISSENSE	T173A	ENST00000339953
CLU	8:27462818	T	C				0.40	MISSENSE	Y13C;Y151C;Y151C;Y151C;Y162C;Y203C	ENST00000522098;ENST00000316403;ENST00000405140;ENST00000523500;ENST00000546343;ENST00000560366
CRTC3	15:91136959	G	A				0.28	MISSENSE	R108Q;R108Q	ENST00000420329;ENST00000268184
DENND5A	11:9187435	G	A				0.24	MISSENSE	A744V;A744V	ENST00000530044;ENST00000328194
FAT3	11:92531707	C	A				0.29	MISSENSE	T1843N;T1843N	ENST00000409404;ENST00000298047
GALNT15	3:16237365	G	A				0.17	MISSENSE	S213N	ENST00000339732
GPAM	10:113926232	T	A				0.32	MISSENSE	R383S;R383S	ENST00000348367;ENST00000423155
GPR19	12:12814555	C	A				0.32	MISSENSE	K276N;K276N	ENST00000332427;ENST00000540510
GRIN2C	17:72848207	C	T				0.50	MISSENSE	G315R;G315R	ENST00000293190;ENST00000347612
GRM5	11:88300504	T	A				0.15	MISSENSE	I783F;I783F;I783F;I783F;I783F	ENST00000305432;ENST00000455756;ENST00000305447;ENST00000418177;ENST00000393297
IKZF3	17:37944604	A	G				0.43	MISSENSE	F206L	ENST00000346872
KAT6B	10:76748818	G	T				0.34	MISSENSE	M567I;M567I;M567I;M676I;M859I	ENST00000372714;ENST00000372724;ENST00000372725;ENST00000372711;ENST00000287239
KAT8	16:31129052	T	G				0.24	MISSENSE	V17G;V17G	ENST00000219797;ENST00000543774
LCN2	9:130912557	C	T				0.21	MISSENSE	A60V;A60V;A60V;A60V	ENST00000277480;ENST00000373017;ENST00000540948;ENST00000372998
MBD5	2:149243412	C	T				0.33	NONSENSE	Q1216*;Q983*	ENST00000404807;ENST00000407073
MLC1	22:50506954	T	C				0.18	MISSENSE	T268A;T268A	ENST00000311597;ENST00000395876
MTCH2	11:47660279	C	G				0.16	MISSENSE	G84A	ENST00000302503
NCAM1	11:113130901	C	A				0.40	MISSENSE	P535T	ENST00000533760
NME6	3:48336688	C	G				0.42	MISSENSE	A91P;A91P;A91P;A91P	ENST00000415053;ENST00000426689;ENST00000442597;ENST00000452211
OR5K3	3:98109571	C	G				0.45	MISSENSE	P21R	ENST00000383695
PBRM1	3:52610704	CTTT	C				0.37	CODON_DELETION	K1149-;K1181-;K1181-;K1181-;K1196-	ENST00000356770;ENST00000337303;ENST00000409057;ENST00000296302;ENST00000409114
PRR23A	3:138724387	T	C				0.44	MISSENSE	S242G	ENST00000383163
SLAMF1	1:160604564	G	A				0.17	MISSENSE	A180V;A180V;A180V;A180V	ENST00000538290;ENST00000355199;ENST00000235739;ENST00000302035
SYNE2	14:64469762	A	C				0.28	MISSENSE	K1371Q;K1371Q	ENST00000344113;ENST00000358025
TCTN1	12:111085632	G	A				0.28	MISSENSE	G567S;G572S	ENST00000551590;ENST00000397659
TEKT2	1:36553091	G	T				0.18	MISSENSE	D303Y	ENST00000207457
TMEM110	3:52931397	C	T				0.15	MISSENSE	A24T;A24T	ENST00000355083;ENST00000504329
ZNF860	3:32031478	A	C				0.17	MISSENSE	S303R	ENST00000360311